XIX CONGRESSO NAZIONALE SIES2026
Firenze | 4-6 marzo 2026
Palazzo degli Affari

XIX Congress of the Italian Society of Experimental Hematology ABSTRACT N. CO23

Monoclonal Gammopathies & Multiple Myeloma

SPATIAL IMAGING UNLOCKS THE POTENTIAL OF CHARTING MULTIPLE MYELOMA AND EXTRAMEDULLARY DISEASE

V. Desantis[1], A. Andriano[1], G. De Martino[1], T. Düking[2], O. Hartwig[2], G. Ingravallo[3], M. Biondo[4], C. Botta[5], R. Ria[6], A. Vacca[6], A.G. Solimando[6]

[1]Department of Precision and Regenerative Medicine and Ionian Area-DiMePRe-J, Section of Pharmacology, University of Bari Aldo Moro Medical School; [2]Miltenyi Biotec B. V. & Co. KG; [3]Pathological Anatomy Unit, Department of Emergency and Organ Transplantation, University of Bari Aldo Moro; [4]Department of General Surgery and Medical-Surgical Specialties, University of Catania; [5]Department of Health Promotion, Mother and Child Care, Internal Medicine and Medical Specialties, University of Palermo; [6]Internal Medicine Guido Baccelli, University of Bari Aldo Moro Medical School, Italy

Introduction: Multiple myeloma (MM) is a plasma cell (PCs) cancer marked by strong genetic, phenotypic, and microenvironmental heterogeneity. The emergence of extramedullary disease (EMD) signals an aggressive phase linked to treatment resistance and poor outcomes. The mechanisms driving plasma cells to escape the bone marrow and infiltrate extramedullary sites remain unclear. This study uses MACSima™ imaging cyclic staining (MICS), a high-dimensional spatial imaging technology, to map protein expression patterns and cellular interactions, revealing structural and network differences between bone marrow and EMD lesions.

Methods: Using MICS, researchers stained 56 biomarkers across carefully prepared BM and EMD tissue samples from 5 newly diagnosed MM patients. Data from 231,186 cells were analysed, with 105,047 annotated as PCs. Computational tools processed and statistically validated the imaging data to generate spatial maps and cellular profiles. Distinct clustering patterns of PCs and immune infiltration profiles were identified via cell-type heatmaps and spatial distance analyses. This approach allowed for comprehensive 3D mapping of malignant PCs and key tumor microenvironment components, providing an integrated spatial framework for investigating cellular organization and intercellular interactions.

Results: MICS technology enabled the identification of 14 distinct cell types in BM and 9 in EMD, showcasing method's capacity to discern cellular diversity at a single-cell level. EMD lesions displayed disrupted architecture, characterized by a loss of stromal network integrity and diminished crosstalk with regulatory immune cells. Malignant PCs in EMD sites were organized into dense clusters, lacking canonical interactions with $CD8^+$ T cells and dendritic cells, indicative of an immunologically permissive microenvironment. PCs at EMD sites exhibited higher expression of drug resistance markers like BCL-2 and EZH2, and reduced CD38 expression, confirmed by immunohistochemistry. The spatial arrangement of immune cells such as T-cells and macrophages, was markedly different in EMD compared to BM. PCs were overall far distant from T-cells in EMD (Figure1_Desantis).

Conclusions: This study provides the first evidence that spatial imaging is essential for understanding the structural complexity of MM and its progression to EMD. Three-dimensional reconstruction of cellular networks reveals the loss of immunostromal interactions and the formation of protective niches that sustain highly aggressive plasma cell subclones. This may explain the reduced effectiveness of CD38-targeted and immune-mediated therapies (such as CAR-T and bispecific antibodies) in EMD. Although larger studies are needed to confirm these findings, they offer valuable insights for precision medicine and microenvironment-focused strategies that could transform the treatment of MM with an extramedullary phenotype.

Acknowledgements: This work was supported by "Fondo per il Programma Nazionale di Ricerca e Progetti di Rilevante Interesse Nazionale-PRIN" (project n.2022ZKKWLW); by the Italian network of excellence for advanced diagnosis (INNOVA) (code PNC-E3-2022-23683266 PNC-HLS-DA), by PNRR-MCNT1-2023-12377893 DEMMMO (code H93C23001080006), by Complementary National Plan PNC-I.1 DARE-DigitAl lifelong pRevEntion initiative (code PNC0000002, CUP B53C22006420001) and by AIRC within My First AIRC Grant 2020 (n. 24534, 2021/2025).

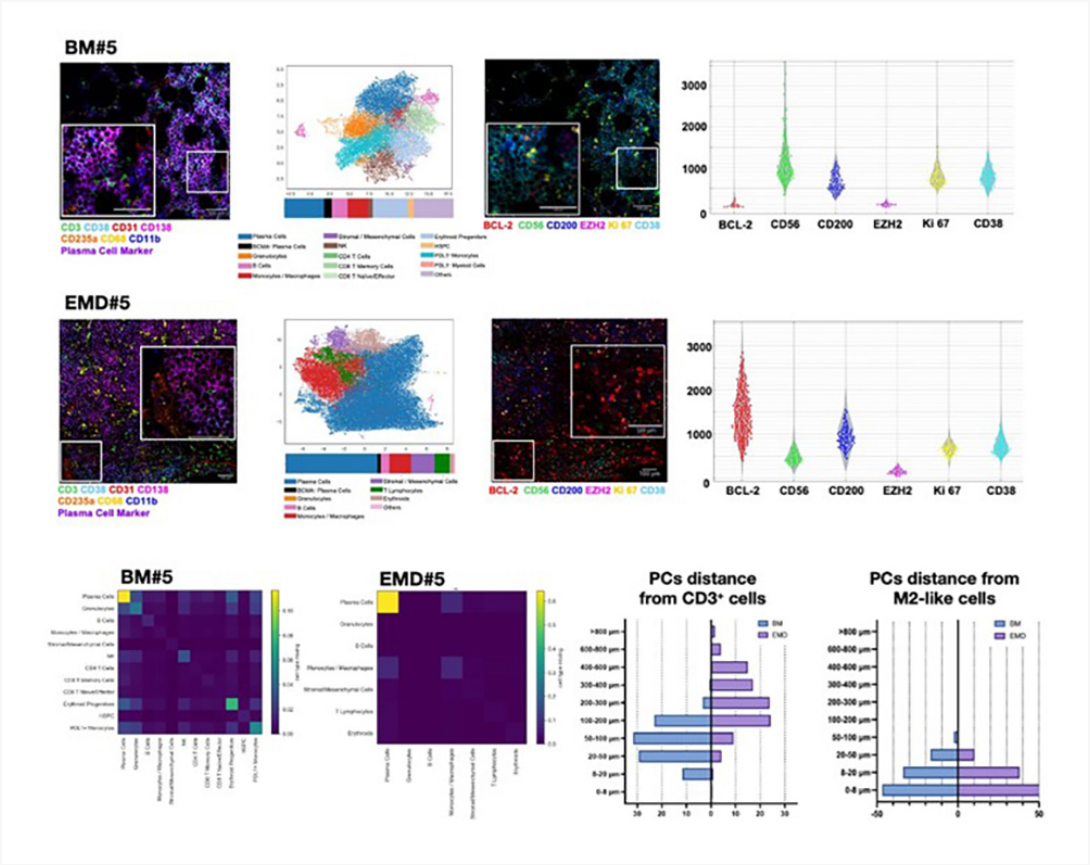
BM#5
CD3 CD38 CD31 CD138
CD235a CD45 CD11b
Plasma Cell Marker
BCL-2 CD56 CD200 EZH2 Ki 67 CD38
3000
2000
1000
0
BCL-2
CD56
CD200
EZH2
Ki 67
CD38
EMD#5
CD3 CD38 CD31 CD138
CD235a CD45 CD11b
Plasma Cell Marker
BCL-2 CD56 CD200 EZH2 Ki 67 CD38
3000
2000
1000
0
BCL-2
CD56
CD200
EZH2
Ki 67
CD38
BM#5
EMD#5
PCs distance from CD3+ cells
PCs distance from M2-like cells